6-1-2007

Intermittent PTH Treatment of ICER Transgenic Mice

Jill R. Danaher

Intermittent PTH treatment of ICER transgenic mice

Jill Randall Danaher

BA, Albertus Magnus College, 1992

DMD, University of Connecticut, 1997

A thesis

submitted in the partial fulfillment of the

requirements for the Degree of

Master of Dental Science

at the

University of Connecticut

2007

Approval Page

Master of Dental Science Thesis

Intermittent PTH treatment of ICER transgenic mice

Presented by

Jill Randall Danaher, DMD

Major Advisor _____
Barbara E. Kream, PhD

Associate Advisor _____
John Harrison, PhD

Associate Advisor _____
Sunil Wadhwa, DMD, PhD

Associate Advisor _____
Flavio A. Uribe, DDS, MDS

University of Connecticut

2007

Table of Contents

List of Figures

Introduction

Parathyroid hormone (PTH) is the major calcium-regulating hormone in humans. In addition to its actions on calcium metabolism, decades of animal and human studies have shown that PTH can be a potent anabolic agent when administered intermittently. Currently, it has been Food and Drug Administration approved for the management of post-menopausal and idiopathic osteoporosis. In bone, PTH binds to PTH1R receptors on osteoblasts, initiating three molecular cascades: an increase in intracellular calcium, and the activation of the protein kinase C (PKC) and protein kinase A (PKA) pathways. The anabolic effect of PTH on bone mass acquisition is mediated by the PKA signaling pathway. However, the exact molecular mechanisms of PTH signaling are complex and still not fully understood.

Our laboratory examines the role of the cAMP responsive element modulator (*Crem*) gene, a member of the basic leucine zipper (bZIP) ATF/CREB family of transcription factors, in the PTH anabolic response. The Crem gene encodes the inducible cAMP early repressor (ICER), which acts as a dominant regulator of gene transcription because it contains essentially only the DNA binding domain of CREM [1]. Previous studies demonstrated that PTH rapidly and transiently induces ICER in osteoblastic cells via the PKA pathway [2, 3].

To better understand the role of ICER, Huang et al developed transgenic mice with osteoblast-targeted expression of ICER[4]. These transgenic mice have low bone mass, impaired osteoblast differentiation and increased osteoclast precursors in bone

marrow. This mouse model suggests that the ICER transgene disrupts the activity of ATF/CREB factors required for normal bone remodeling [4]. Further study is needed to determine the in vivo specificity of ICER protein, including if in the presence of an induced anabolic stimuli ICER has the sole ability to disrupt bone mass acquisition.

Parathyroid hormone

Parathyroid hormone (PTH) is secreted by the parathyroid glands in response to changes in serum calcium (4). More specifically, there are calcium receptors on the parathyroid glands which regulate the feedback loop between PTH and serum calcium levels. It is PTH which acts to balance both bone resorption and bone formation. PTH binds to PTHR1 receptors on the surface of osteoblasts and engages three signaling pathways: PKA, PKC and intracellular calcium (**Figure 1**).

The PKA pathway involves the formation of cAMP, the binding of cAMP to the regulatory subunit of PKA, which then releases the active catalytic subunits [5]. These subunits then translocate to the nucleus and phosphorylate the transcription factor CREB (cAMP response element binding protein), leading to the expression of cAMP-inducible genes [6].

The unique anabolic ability of PTH to stimulate activation of remodeling units, which enhance bone formation over resorption, has led to the growing interest in the therapeutic efficacy of PTH [7]. Currently, parathyroid hormone (PTH) is approved for the management of post menopausal and idiopathic osteoporosis. Decades of

animal and human studies of PTH have discovered that variables such as dosing regimens, duration of treatment and dose magnitude determine if the effects will be anabolic or catabolic[8]. However, the exact mechanisms of PTH's action are complex and not yet fully understood. A clearer understanding of the molecular mechanisms responsible for the anabolic action of PTH on both cortical and trabecular bone will aid in designing better treatment options.

PTH has been shown to be an effective anabolic agent in humans, rats, rabbits and primates when administered intermittently [7-9]. Clinical studies in humans have found the anabolic effects of PTH to be both time and dose dependent. The use of PTH(1-34) or PTH(1-84) results in a peak serum concentration of approximately 60 to 120 minutes and a disappearance at 6 to 8 hours [7]. At least three randomized clinical studies found that from daily PTH injections there is a significant increase in bone mineral density at trabecular bone sites, that bone remodeling is enhanced with markers of bone formation rising early followed by an increase in bone resorption, and that bone strength increases by way of greater trabecular, cortical and overall bone volume[7]. In these trials, daily subcutaneous injections of PTH increased spinal bone mass density by only 8-10%. Bone mineral density increases in the femur and total body were considerably less ranging from 3-5% and radial bone mineral density either declined slightly or remained the same when measured by dual X-ray energy absorptometry [7]. The more significant finding was a time-dependent marked fracture risk reduction even in sites that showed no increases in bone mineral density [7]. Also, suggesting a change in the quality of bone.

The most common animal model used has been the ovariectomized animal, which closely resembles the skeletal loss due to estrogen deprivation seen in postmenopausal humans. In this model, it was discovered that intermittent PTH prevented the 50% trabecular bone volume loss post ovariectomy and increased bone formation by increasing bone apposition on the periosteal and endosteal surfaces, while intracortical bone was renewed through remodeling [7, 8]. More studies have examined the skeletal effects of PTH therapy but only a few studies have looked at the effects in oral osseous tissue in the aged ovariectomized rat model. After an intermittent PTH protocol (5 days a week for 10 weeks), Miller et al found no effect on dentin formation from the incisors but most indices of bone formation, including the double-labeled surface, mineralizing surface, mineral appositional rate, new bone area and surface-referent bone formation rates, were greater in the PTH-treated group compared with both the Ovx and the Sham controls measured at the periosteal and cancellous bone surfaces of the mandible [10].

More recently, the mouse model has been used to study the anabolic effects of PTH at the molecular level. An advantage of using this model is the ability to genetically alter the mouse and study the effects of anabolic agents at the molecular level. In 2002, Iida-Klein et al, studied how bone mineral density changes with age in the murine skeleton of C57BL/6J mice, when peak bone mass is achieved and whether there are any site-specific effects of intermittent PTH treatment [11]. They found that with daily PTH injections, there was an increase of gene expression in bone formation and resorption in the post-adolescent female mouse and that bone mineral density

increased at all sites including the tibia, femur, and total body. These results are similar to the above actions of PTH observed in humans and rats and, thus, demonstrate that it is a viable model in which to study the anabolic effects of PTH.

Inducible cAMP Early Repressor

The cAMP responsive element modulator (CREM) gene, is a member of the CREB/ATF family of basic leucine zipper transcription factors [2]. This gene gives rise to multiple proteins by alternative splicing of the CREM transcript and using alternative promoters [3]. These proteins function as transcriptional activators or repressors by binding to cAMP response elements (CREs). In 1993, Molina et al, identified and characterized one such protein called the inducible cAMP early repressor (ICER)[1].

ICER transcripts are transcribed from the intronic promoter P2 of the CREM gene. By alternative splicing, four isoforms are transcribed: I, I gamma, II, and II gamma [1, 3] (**Figure 2**). ICER proteins contain a unique N-terminal amino acid sequence and either DNA binding domains (DBD) I or II but lack the kinase-inducible domains of CREM. Thus, ICER proteins in most cases act as transcriptional repressors [3].

The functions of ICER are two-fold: to inhibit transcription of cAMP-induced transcription by binding to promoter sequences or by forming inactive heterodimers with other bZip transcription factors [1]; ICER also has the unique ability to regulate

its own transcription by binding to the CARE site, two pairs of clustered cAMP response elements, in the P2 promoter of the CREM gene (**Figure 3**).

While PTH is known to induce multiple gene expression in osteoblasts, Tetradis et al specifically, examined whether PTH induced the ICER protein. They showed that PTH did induce all known ICER transcripts in MC3T3-E1 cells and neonatal mouse calvariae with mRNA levels peaking at 2 to 4 hours and declining to baseline by 10 hours [3]. Thus, ICER's expression is characterized as rapid and transient.

In a later study, the pathways through which PTH induces ICER; these could be PKC, PKA and/or calcium influx) [2]. Their results revealed that only agents that signal through the cAMP-PKA pathway were able to induce ICER and positive and negative manipulation of this pathway significantly effected ICER expression.

Transgenic Mouse Model

In an effort to study to the functions of ICER in vivo, Huang et al developed a transgenic mouse with osteoblast-targeted expression of ICER [4]. The pOBCol3.6-ICER I and II transgenes were constructed by cloning ICER I and ICER II cDNAs, each containing an N-terminal FLAG epitope tag, downstream of a fragment containing a 3.6-kb fragment of the rat Colla1 promoter and most of the rat Colla1 first intron. Four lines of transgenic mice in the CD-1 background were generated by embryo microinjection.

Of all the ICER I transgenic lines tested, line 284 has the highest transgene mRNA expression in bone [4]. This line has lower body weight and decreased bone mineral density (determined by DEXA) than wild-type littermates. Serum osteocalcin, a marker of bone formation, was reduced in the serum of transgenic mice. Furthermore, histological sections of distal femurs showed almost no trabecular bone, and histomorphometry showed a significant reduction in percent trabecular bone volume. Dynamic histomorphometry revealed a significant decrease in the mineral apposition rate (MAR) and bone formation rate per bone surface (BFR/BS).

Microcomputed tomography (microCT) was done to assess bone morphometry. Three dimensional images of femoral sections revealed a dramatic reduction in the trabecular bone compartment. Accordingly, morphometic analysis showed a reduction in trabecular bone volume, number and thickness. Cross-sectional images through the mid-diaphaseal region of femurs showed a significant decrease in cortical bone area and thickness. Additionally, in a subsequent unpublished study performed in our laboratory, microCT of the ICER transgenic mandibles revealed a mark reduction in bone volume with respect to total bone volume, generalized pitting of bone and a statistically significant reduction in cortical tissue density [12].

To examine the effect of the ICER transgene on osteoblast differentiation, a green fluorescent protein (GFP) transgene (pOBCol2.3-GFP) was bred into the ICER mice as a marker of late osteoblast differentiation [4]. They showed that bone marrow cultures from ICER mice had impaired osteoblast differentiation. Although osteoclast

number per bone surface was not significantly altered in femoral trabecular bone from ICER mice, osteoclast precursors were increased 2-fold in the transgenic bone marrow cultures. Thus, these collective results indicate that the low bone mass in transgenic mice with osteoblast-targeted ICER expression was caused by a dysregulation of both bone formation and resorption. This transgenic model suggests that ICER disrupts molecular pathways that are critical for normal bone remodeling.

Significance and Rationale of Research

PTH (1-34) is currently FDA approved and being effectively used in osteoporosis [7]. While antiresorptive agents are used to increase the mineral content of existing bone, they cannot cause an increase in bone mass [9]. However, when administered intermittently PTH can build both cortical and trabecular bone [8]. The treatment protocol requires single daily injections and is not without disadvantages such as cost, compliance and even potential risk of malignant transformation [7]. Despite its use, the exact mechanisms responsible for the anabolic actions of PTH are still not fully understood. Identification of these molecular mechanisms, will aid in the design of better treatment options, not just for the treatment of post-menopausal osteoporosis but for other metabolic bone diseases.

Our current understanding of the molecular mechanisms on osteoblast cell is that the binding of PTH to osteoblasts induces three molecular cascades: extracellular calcium influx, activation of the PKC pathway and activation of the PKA pathway [5]. Induction of the PKA pathway leads to induction of cAMP inducible genes.

Furthermore, previous studies have found that the cAMP signaling pathway induces ICER expression in many cell types which then represses cAMP-induced transcription of other genes including its own transcription [1].

In 1998, Tetradis et al studied the effects of PTH on osteoblastic MC3T3-E1 cells and mouse calvarie and found that it rapidly and transiently induced ICER mRNA[3]. A subsequent study, found that only manipulation of the cAMP-PKA signaling pathway affected the expression of ICER mRNA and protein [2]. In addition, the osteopenia in the transgenic mice with osteoblast-targeted overexpression of ICER suggests that ICER disrupts the molecular pathways that govern normal bone remodeling [4]. Therefore, we believe in vivo that PTH-induced ICER is a physiological regulator of downstream target genes. In ICER transgenic mice, thus, the response of bone to PTH should be blocked.

Objective of Research

The goal of this research was to determine whether ICER transgenic mice have an altered response to an intermittent PTH treatment protocol. Previous studies have shown that PTH and cAMP induce ICER gene expression in osteoblasts and that the anabolic effect of PTH is mediated by the cAMP-PKA pathway [2]. Our objective was to determine if ICER overexpression will prevent the acquisition of bone mass by intermittent PTH treatment.

Specific Aim

The aim of this study was to examine bone density, morphology and cellular response of ICER transgenic mice to an intermittent PTH injection protocol. This involved injection of wild type and ICER transgenic mice 5 times per week for four weeks with 80 μg/kg of PTH. Bone mass, bone micro-architecture and osteoblast activity were then measured by DEXA, micro CT, serum osteocalcin levels and dynamic histomorphometry.

Hypothesis

An anabolic PTH treatment protocol in ICER transgenic mice does not increase bone mass.

Materials and Methods

Mice

The cohorts of mice used consisted of 20 female, 10- to 11-week-old CD-1 wild-type mice and 17 female, 10- to 11-week-old line 284 ICER transgenic mice. The groups were derived from four different breeding units (**Figure 4**). All mice were divided into four treatment groups: wild-type PTH-treated, wild-type vehicle-treated, ICER transgenic PTH-treated, and ICER transgenic vehicle-treated. All animal protocols were approved by the institutional Animal Care and Use Committee (protocol #2006-215).

Pre-experimental Measurements

Weight

Total body weights of all mice were recorded using a digital scale.

Anesthesia

Mice were anesthetized using a precision vaporizer that supplied isoflurane at a desired concentration in pure oxygen flow (1.5-2% isoflurane with 250 ml/min O_2).

Bone Mineral Density

To determine baseline whole body bone mineral density, each mouse (under anesthesia) was subjected to a PIXImus Dual Energy X-ray Absorptiometry (DEXA) densitometer (Lunar Corporation, Madison, WI). The machine was initially calibrated with a phantom of a defined value.

Preparation of PTH and Vehicle Solutions

Human PTH(1-34) (Bachem Bioscience Inc, King of Prussia, PA, USA) was dissolved in 1 mg/ml BSA/0.01 N HCl (vehicle) to prepare a dosing solution. Mice were injected with vehicle or PTH. Mice received a final dosage of 80 μg/kg of PTH. The concentration of the dosing solution was determined from the average weight of the wild-type mice and transgenic mice.

Injection Protocol

Human PTH(1-34) solution and vehicle solution was injected once daily for 5 consecutive days, then 2 days off, for 4 weeks. Subcutaneous injections between the scapulas were done with a small 27-gauge needle using a 0.5 ml insulin syringe. The injection volume for wild type mice was 0.050 ml while the injection volume for transgenic mice was reduced by the percentage average body weight difference compared to wild-type mice (usually about 30%). As mentioned above, all mice received the same dose of PTH based on body weight.

Markers for Bone Labeling

Ten days prior to sacrifice, all mice were injected with calcein intraperitoneally (Sigma, St. Louis, MO) at 10 mg/kg body weight with a small 27-gauge needle using a 0.5 ml insulin syringe. Then, two days prior to sacrifice, mice were injected intraperitoneally with xylenol orange (Sigma, St. Louis, MO) at 90 mg/kg body weight.

Experimental Endpoint Measurements

Weight

At 14-15 weeks (end of the experiment), total body weight was recorded on a digital scale. Mice were sacrificed by CO_2 asphyxiation followed by cervical dislocation.

Serum Bone Turnover Markers

Blood was obtained by cardiac puncture. Samples were allowed to clot for at least 30 minutes and then centrifuged for 10 minutes at 1,000 x g. Serum was removed immediately and stored at -20 degrees C. Serum osteocalcin was measured by radioimmunoassay using a goat anti-mouse osteocalcin antibody [13] by Dr. Caren Gundberg of the Yale University Core Center for Musculoskeletal Disorders. The C-terminal telopeptide of α1(I) collagen was measured by an enzyme-linked immunosorbent assay (ELISA) using a RatLaps kit (Nordic Bioscience Diagnostics, A/S).

Bone Mineral Density

Mice underwent full body DEXA to determine post-experimental whole body bone mineral density. The machine was initially calibrated with a phantom of a defined value.

MicroCT

Dissected femurs, L3 vertebrae and hemi-mandibles (bisected at the symphysis) were fixed in 70% ethanol and analyzed by MicroCT. Trabecular morphometry within the

metaphyseal region of distal femurs and the centrum of the third lumbar vertebrae was quantified using microCT (μCT40, Scanco Medical AG, Bassersdorf, Switzerland). Three-dimensional images were reconstructed using standard convolution back-projection algorithms with Shepp and Logan filtering, and rendered within a 12.3 mm field of view at a discrete density of 578,704 voxels/mm^3 (isometric 12-μm voxels). Segmentation of bone from marrow and soft tissue was performed in conjunction with a constrained Gaussian filter to reduce noise. For volumetric analysis, regions were selected within the endosteal borders to include the central 80% of vertebral height and secondary spongiosa of femoral metaphyses located 960 μm (~6% of length) from the growth plate. Trabecular morphometry was characterized by measuring bone volume fraction (BV/TV, %), connectivity density, surface density (BS/TV), trabecular thickness (TbTh), trabecular number (TbN), and trabecular spacing (TbSp).

Cortical morphometry was also evaluated in femurs using microCT. Three-dimensional images were reconstructed using standard convolution backprojection algorithms with Shepp and Logan filtering, and rendered at a discrete density of 578,704 voxels/mm^3 (isometric 12 μm voxels). Bone was threshold segmented from marrow and soft tissue at an attenuation coefficient of 2.8 cm^{-1}. Cortical morphometry was quantified and averaged for fifty cross sections (600 μm) at the mid-diaphysis, measured between proximal and distal growth plates. Direct measurements of cross-sectional geometry provided subperiosteal area, subendosteal area, and cortical areas. A circular model was applied to the periosteal and

subendoesteal area magnitudes to calculate average values of the cortical width, periosteal and endosteal radii, and periosteal and endosteal perimeters.

A qualitative and quantitative 3-dimensional analysis of hemi-mandibles was performed using microCT. The hemi-mandibles were scanned in cross section from the incisal edge of the incisor to the condyle of the mandible and 12 micron sections were acquired. Analysis was performed at three different locations along the length of the mandible: 1) the alveolar crest, the first section in which the alveolar bone is seen; 2) the level of the first molar at the center of the mesial root; and 3) the level of the third molar, first section in which the second molar cannot be seen. The measurements included bone volume (BV/TV) and tissue density of enamel, labial dentin and lingual dentin of the incisor at all 3 sites mentioned above.

Histomorphometry

Histomorphometry was done to evaluate rates of bone formation and mineralization. L3 vertebrae were put into 70% ethanol, then fixed, dehydrated, cleared, embedded in plastic, and sectioned. The sections were then deplasticized and evaluated by fluorescence microscopy. The measurements were taken at approximately 200 microns from the epiphyseal growth plate. All dynamic parameters were measured according to the Report of the ASBMR Histomorphometry Nomenclature Committee [14].

Statistical Analysis

In the figures, all values shown are the mean ± SD of the number of values indicated. Data between groups was analyzed with unpaired student's t-tests. A p value of <0.05 was considered significant.

Results

Percent Change in Body Weight

Weight was recorded in grams before and after the treatment protocols and the percent change was recorded. The percent change in body weight between the wild-type PTH treated group (14.6±4.8) and the wild-type vehicle treated group (8.2±7.6) was significant. In contrast, the percent increase in body weight was not significant between the ICER transgenic PTH group (13.7±9.4) and the ICER transgenic vehicle group (12.5±17.3) (**Figure 5**).

Bone Mineral Density and Bone Mineral Content

For each group, the percent change in bone mineral density and bone mineral content was analyzed. The wild-type PTH group showed an increasing trend (p=.06) in bone mineral density when compared with the wild-type vehicle group (**Figure 6**). However, the transgenic PTH group did not demonstrate a significant change in bone mineral density compared to the transgenic vehicle group (**Figure** 7). Neither the wild-type nor the transgenic groups had a significant change in bone mineral content.

Serum Osteocalcin

Serum osteocalcin levels were measured after the treatment protocols. There was a significant increase in serum osteocalcin (p=.03) in the wild-type PTH treated group compared to the wild-type vehicle treated group (**Figure 8**). However, serum osteocalcin levels in the transgenic group did not increase after treatment with PTH (**Figure 9**).

Microcomputed Tomography

Femur

The cortical bone of the femurs was the most responsive to PTH treatment. The wild-type group showed a significant change in cortical thickness measured in mm after PTH therapy (**Figure 10**). The transgenic group had an increasing trend (p=.06) in cortical thickness. Interestingly, the TG group did show a significant increase in cortical porosity after PTH treatment which was not seen in the wild-type group (**Figure 11**). Therefore, an examination of the segmented cortical bone area measured in mm^2 was performed to evaluate the cortical bone without the voids. There was a small increasing trend (p=.1) in cortical bone area in the wild-type group after the PTH treatment, and a significant increase in cortical bone area in the transgenic group after PTH treatment (**Figure 12).**

The trabecular bone of the femurs was not very responsive to PTH in our study. No significant changes in trabecular bone volume fraction (BV/TV) were seen in the wild-type or transgenic groups after PTH treatment. However, within the wild-type group, there was a significant increase in trabecular thickness (**Figure 13**). Changes in mean trabecular number and spacing were not significant in either the wild-type or transgenic groups.

Vertebrae

The trabecular bone of the L3 vertebrae had some varied and unexpected responses to PTH treatment. The wild-type group did not respond to the PTH with a significant

increase in trabecular BV/TV. However, there was a significant increase in trabecular BV/TV in the transgenic group after the PTH treatment (**Figure 14**).

Mandible

The 3-dimensional reconstructions of the mandibles showed an obvious bone phenotype in the transgenic mice. The transgenic mandibles showed generalized pitting of the bone and severe loss of alveolar bone around the molars (**Figure 15**). Interestingly, a common finding noted within the transgenic group was the loss of molars. It is unclear if they were lost in the mice in vivo or whether they fell out during dissection and/or analysis. There were, however, no apparent PTH effects on the bone phenotype within the wild-type or transgenic groups.

Cross-sectional, quantitative analyses of cortical bone were performed at the mesial roots of the first and third molars. After PTH treatment, neither the wild-type nor transgenic groups showed a significant increase in BV/TV (**Figure 16**). There was a significant decrease in cortical bone at the 1^{st} molar and 3^{rd} molar regions noted in the transgenic group compared to the wild-type group typical of the ICER transgenic bone phenotype.

Histomorphometry

The dynamic labeling of sectioned L3 vertebrae was evaluated and measured to confirm and extend the microCT analyses. The wild-type group showed a trend ($p=.07$) toward increased mineral apposition rate (MAR) after the PTH treatment;

however, there was no change in the bone formation rate per bone surface (BFR/BS) (**Figures 17 and 18**). In contrast, the transgenic group showed a trend (p=.06) toward increased BFR/BS but not a change in the mineral apposition rate (MAR) (**Figures 19 and 20**).

Discussion

Previous studies have examined the expression of ICER in osteoblasts in vivo and in vitro. Molina et al demonstrated the repressive functions of ICER[1]. Tetradis et al showed that ICER is induced by PTH and cAMP in osteoblastic cells[3]. Later, Nervina, et al showed that the expression of ICER in osteoblasts is coupled to the cAMP-PKA signaling pathway[2]. These findings have led to the hypothesis that ICER induction in osteoblasts acts as a mechanism to regulate cAMP-dependent gene expression, and that it could affect the magnitude or time course of gene expression in response to hormones, such as PTH, that stimulate cAMP production.

To evaluate the in vivo role of ICER in bone, our laboratory has used two mouse models: CREM-knockout mice and transgenic mice with osteoblast-targeted expression of ICER. Lui et al studied the effects of PTH administration in CREM-knockout mice[15]. He showed that CREM deficiency alters the response of bone to PTH such that osteoclastogenesis is increased. This blunts bone mass acquisition in response to PTH treatment. Furthermore, our laboratory developed and characterized a transgenic mouse model with an overexpression of ICER in cells of the osteoblast lineage (pOBCol3.6-ICER) [4]. The osteopenic phenotype suggests that ICER may disrupt bone remodeling.

The present study was designed to examine the response of ICER transgenic bone to an anabolic dosage of PTH. Initial tests to evaluate bone formation did not reveal significant increases in bone mineral density or serum osteocalcin levels. After

evaluating specific bones, we did see increases in bone mass after measuring the femoral cortical bone area and the vertebral trabecular bone volume in the transgenic mouse after PTH treatment. The wild-type responded with a significant increase in femoral cortical thickness, but the wild-type vertebral trabecular bone did not respond to PTH treatment. Our results indicate that there are site specific anabolic responses to PTH in ICER transgenic mice, suggesting that even in the presence of increased ICER protein, there are still selected responses to PTH.

The changes in femoral cortical bone versus trabecular bone found in the wild-type mouse after PTH treatment are consistent with what Wang et al, found in CD-1 mice [16]. Given that the population of this study included only female mice, it is interesting to note that Wang et al also reported that the anabolic response was blunted in female CD-1 mice versus male CD-1 mice. In our study, the significant increase in cortical bone volume and increasing trend in cortical bone area in the wild-type was also reflected in the increasing trend in bone mineral density determined by DEXA and the significant increase in serum osteocalcin levels.

The PTH treatment protocol appeared to induce significant porosity in the femoral cortical bone of the transgenic mice. A response not noted in the wild-type. This is probably indicative of increased osteoclast activity but, of course, it is in need of further study. Regardless, we still noted a trend toward increased femoral cortical thickness and a significant increase in cortical bone area within the transgenic mice.

The fact that the lumbar vertebrae in the wild-type mice did not respond with an increase in bone volume as seen in previous studies using the C57BL/6 black mouse may be due to the mouse strain differences or to the PTH protocol being limited to only 4 weeks [11]. CD-1, an outbred strain, and the C57BL/6, an inbred strain, may have different skeletal site specific responses or dose responses to PTH treatment; this warrants further study. In addition, Iida-Klein et al found C57BL/6 mouse vertebrae had less of an anabolic response than the long bones; moreover, the anabolic effects of PTH on vertebrae were only significant after 7 weeks of treatment[11]. However, after only a 4 week treatment period, we did find a trend toward increased mineral apposition rate (MAR) of the wild-type lumbar vertebrae. This may indicate enhanced osteoblastic activity at the cellular level, but a longer treatment protocol would be needed to study this response further.

The bone phenotype of ICER transgenic mice needs to be considered when analyzing the results. First, this mouse model has almost no trabecular bone in the femur and reduced template in the vertebrae. Second, long term changes in body weight and bone mineral density have yet to be characterized. Third, we noted that the population of ICER transgenic mice varies greatly in terms of body weight percent changes and physical deformities even at the same age. The average percent change in body weight of the transgenic mice was 12 percent but some of the mice had extreme changes such as an increase in body weight by 49 percent or a decrease in body weight by 5.5 percent. Some of the transgenic mice suffered from Kyphosis and/or malpositioned rear feet.

In our study, the transgenic mice did not respond to PTH with a significant increase in full body bone mineral density or serum osteocalcin. Yet, the bone volume fraction (BV/TV) of the lumbar vertebrae was significantly increased. Furthermore, the increased trend in the bone formation rate per bone surface (BFR/BS) of the vertebrae is indicative of a greater number of osteoblasts producing bone, and thus of an increase in bone formation at the tissue level. These findings suggest either skeletal site or dosage specificity within ICER transgenic mice, or that the baseline amount of vertebral bone was sufficient to show an increase. Where as, the femoral trabecular bone template may have been too limited to demonstrate such an increase.

The fact that the PTH protocol did not have a significant effect on mandibular bone of the wild-type or the transgenic groups may be due, again, to treatment time, dosage or site-specificity within the murine breed. However, Miller, et al showed significant PTH effects in the mandible; the treatment protocol of 80 micrograms per kilogram of body weight lasted longer, 10 weeks versus 4 weeks, and was given to ovariectomized rats. A literature search does not reveal any published studies on the effects of PTH on the mandibular bone in CD-1 mice.

Conclusion

We hypothesized that ICER would block bone mass acquisition in the presence of an anabolic treatment protocol of PTH, but our experiment suggests that ICER transgenic mice maintain selected responses to PTH. Further, the fact that ICER transgenic mice responded with an anabolic response in the trabecular bone of the vertebrae which was not seen in the wild-type mice demonstrates a site-specific PTH response in this particular mouse model. However, it is still unclear the exact magnitude of ICER's effects on cAMP induced gene expression by PTH. Perhaps, PTH anabolic gene expression occurs by a molecular pathway other than the PKA pathway, or that other CREM/CREB/ATF family products are involved in the anabolic response to PTH.

To better understand ICER's effects in the presence of PTH in the ICER transgenic mice, future study is needed. First, a study is needed to compare the responses of C57BL/6 and CD-1 mice to PTH including various skeletal sites, dosages and time courses. Second, analysis of the osteoclast activity is needed to evaluate the trend in increased femoral cortical porosity after PTH treatment in the ICER transgenic mice. Third, due to the variable changes in body weight and findings of skeletal deformities seen amongst the ICER transgenic population, pre-treatment in vivo microCT would allow us to observe skeletal changes over time in individual mice.

In the future, we will need to generate and evaluate an ICER specific knockout mouse. Collectively, data from the three mouse models should allow us to better characterize ICER's role in bone.

Figure Legend

Figure 1: Osteoblastic cell signaling mediated by PTH. Figure 1 is from Swarthout, J.T., et al., *Parathyroid hormone-dependent signaling pathways regulating genes in bone cells.* Gene, 2002. **282**(1-2): p. 3. PTH binds to PTHR1 receptors on the surface of osteoblasts and engages three signaling pathways: PKA, PKC and intracellular calcium.

Figure 2: Diagram of the *Crem* gene and ICER isoforms. The ICER protein is transcribed at the P2 promoter of the *Crem* gene. Four ICER isoforms (I, I gamma, II, II gamma)are produced from the alternative splicing of either or both the gamma domain and DNA binding domain I. The Diagram was kindly provided by Taranpreet Chandhoke.

Figure 3: The role of ICER in the regulation of gene expression by cAMP. Figure 9 is from Molina, C.A., et al., *Inducibility and negative autoregulation of CREM: an alternative promoter directs the expression of ICER, an early response repressor.* Cell, 1993. **75**(5): p. 886. The schematic demonstrates that the function of ICER via the PKA pathway is two-fold. ICER inhibits transcription of cAMP-induced genes by binding to cAMP response elements (CREs). It also has the unique ability to regulate its own transcription by binding to CARE sites, two pairs of clustered cAMP response elements, in the P2 promoter of the *Crem* gene.

Figure 4: Number of mice and breeding units. The table shows the study population and the breeding units from all 4 experiments: 10 wild-type PTH treated mice, 10 wild-type vehicle treated mice, 10 transgenic PTH treated mice and 7 transgenic vehicle treated mice.

Figure 5: Percent change in body weight. The graph demonstrates that the percent change in body weight between the wild-type PTH treated group (14.6±4.8) and the wild-type vehicle treated group (8.2±7.6) was significant. In contrast, the percent increase in body weight was not significant between the ICER transgenic PTH group (13.7±9.4) and the ICER transgenic vehicle group (12.5±17.3).

Figure 6: Wild-type percent change in bone mineral density. The graph demonstrates an increasing trend (p=.06) in percent change in full body bone mineral density between the wild-type vehicle group (n=7, 1.45±2.92) and the wild-type PTH group (n=6, 5.31±3.55).

Figure 7: Transgenic percent change in bone mineral density. The graph demonstrates no percent change in full body bone mineral density between the transgenic vehicle group (n=6, mean 4.35±4.48) and the transgenic PTH group (n=5, 2.83±3.72).

Figure 8: Wild-type serum osteocalcin levels. The graph demonstrates a significant (p=.03) increase in serum osteocalcin levels between the wild-type vehicle group (n=6, 50.83±10.68) and the wild-type PTH group (n=6, 62.83±14.4).

Figure 9: Transgenic serum osteocalcin levels. The graph demonstrates no change in serum osteocalcin levels between the transgenic vehicle group (n=6, 35.5±6.98) ant the transgenic PTH group (n=5, 38.8±10.78).

Figure 10: Microcomputed tomography analysis of femoral cortical thickness. Microcomputed tomography through the mid-diaphysis of the femur showed a significant increase in cortical thickness measured in millimeters between the wild-type vehicle group (n=10, 0.256±0.01) and the wild-type PTH group (n=10, 0.274±0.01). There was an increasing trend (p=.06) in cortical thickness noted between the transgenic vehicle group (n=6, 0.195±0.003) and the transgenic PTH group (n=10, 0.230±0.03).

Figure 11: Microcomputed tomography analysis of cortical porosity. Microcomputed tomography through the mid-diaphysis of the femur showed a significant (p=.05) increase in porosity (%) of the cortical bone between the transgenic vehicle group (n=6, 3.4±2.8) and the transgenic PTH group (n=10, 6.7±2.9). Cortical porosity did not change between the wild-type vehicle group (n=10, 1.6±1.1) and the wild-type PTH group (n=10, mean 2.4±1.1).

Figure 12: Microcomputed tomography analysis of femoral cortical bone area. Microcomputed tomography through the mid-diaphysis of the femur showed an increasing trend (p=0.1) in cortical bone area (mm^2) between the wild-type vehicles group (n=10, 0.992±0.094) and the wild-type PTH group (n=10, 1.052±0.061). The increase in cortical bone area (mm^2) was significant (p=.03) between the transgenic vehicle group (n=6, 0.803±0.091) and the transgenic PTH group (n=10, 0.935±0.130).

Figure 13: Microcomputed tomography analysis of femoral trabecular thickness. Trabecular morphometry within the metaphyseal region of the distal femur showed a significant increase in trabecular thickness (μm) between the wild-type vehicle group (n=10, 60±6) and the wild-type PTH group (n=10, 69±9). The change in femoral trabecular thickness (μm) was not significant between the transgenic vehicle group (n=6, 55±25) and the transgenic PTH group (n=10, 46±20).

Figure 14: Microcomputed tomography analysis of vertebral trabecular bone fraction. Analysis of trabecular bone volume (BV/TV%) revealed a significant increase between the transgenic vehicle group (n=6, 5.6±2.0) and the transgenic PTH group (n=10, 7.7±2.2). The change in trabecular bone volume between the wild-type vehicle group (n=10, 24.9±3.8) and the wild-type PTH group (n=10, mean 27.4±6.8) was not significant.

Figure 15: Analysis of bone and tooth architecture by microcomputed tomography analysis. Comparison of three dimensional microCT images of wild-type vehicle treated mandibles and transgenic vehicle treated mandibles showed an overall view of the bone and tooth architecture typical of the ICER transgenic phenotype: generalized pitting of the bone and severe loss of alveolar bone around the molars. No apparent PTH effects on the bone phenotype within the wild-type or transgenic groups were noted.

Figure 16: Microcomputed tomography analysis of cortical bone volume fraction at the level of the 1st molar. Cross-sectional, quantitative analysis of the mandibular cortical bone volume (BV/TV%) at the mesial root of the first molar demonstrated no change between the wild-type vehicle group (n=7, 91.1±1.9) and the wild-type PTH group (n=6, 91.6±1.6). There was no change between the transgenic vehicle group (n=6, 74.7±10.2) and the transgenic PTH group (n=5, 72.0±11.6).

Figure 17: Dynamic histomorphometry analysis of wild-type vertebral mineral apposition rate. Quantitative analysis of dynamically labeled and sectioned L3 vertebrae showed a trend (p=.07) toward increased mineral apposition rate (MAR) between the wild-type vehicle group (n=7, 1.38±0.11) and the wild-type PTH group (n=6, 1.54±0.18).

Figure 18: Dynamic histomorphometry analysis of wild-type vertebral bone formation rate per bone surface. Quantitative analysis of dynamically labeled and

sectioned L3 vertebrae showed no change in the bone formation rate per bone surface (BFR/BS) between the wild-type vehicle group (n=7, 0.364±0.100) and the wild-type PTH group (n=6, 0.415±0.100).

Figure 19: Dynamic histomorphometry analysis of transgenic vertebral bone formation rate per bone surface. Quantitative analysis of dynamically labeled and sectioned L3 vertebrae showed a trend (p=.06) toward increasing bone formation rate per bone surface (BFR/BS) between the transgenic vehicle group (n=6, 0.465±0.152) and the transgenic PTH group (n=5, 0.662±0.146).

Figure 20: Dynamic histomorphometry analysis of transgenic vertebral mineral apposition rate. Quantitative analysis of dynamically labeled and sectioned L3 vertebrae showed no change in mineral apposition rate (MAR) between the transgenic vehicle group (n=6, 1.48±0.38) and the transgenic PTH group (n=5, 1.82±0.26).

Figure 1

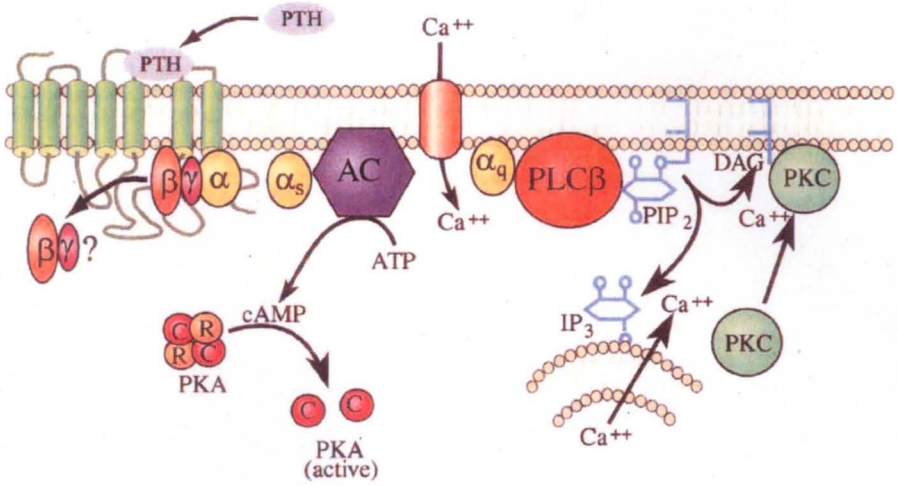

Fig. 1. Osteoblastic cell signaling mediated by PTH.

Figure 1 from Swarthout, J.T., et al., *Parathyroid hormone-dependent signaling pathways regulating genes in bone cells.* Gene, 2002. **282**(1-2): p. 3.

Figure 2

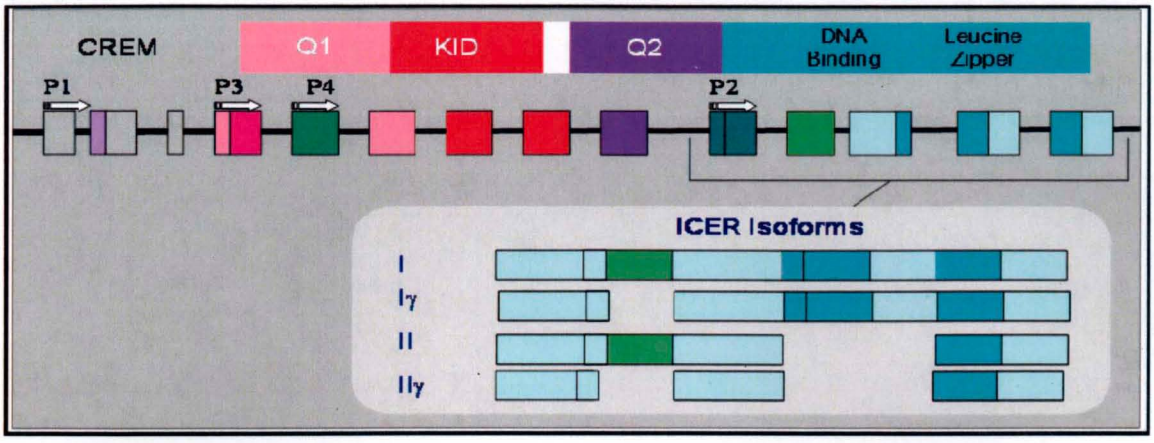

Diagram kindly provided by Taranpreet Chanhoke.

Figure 3

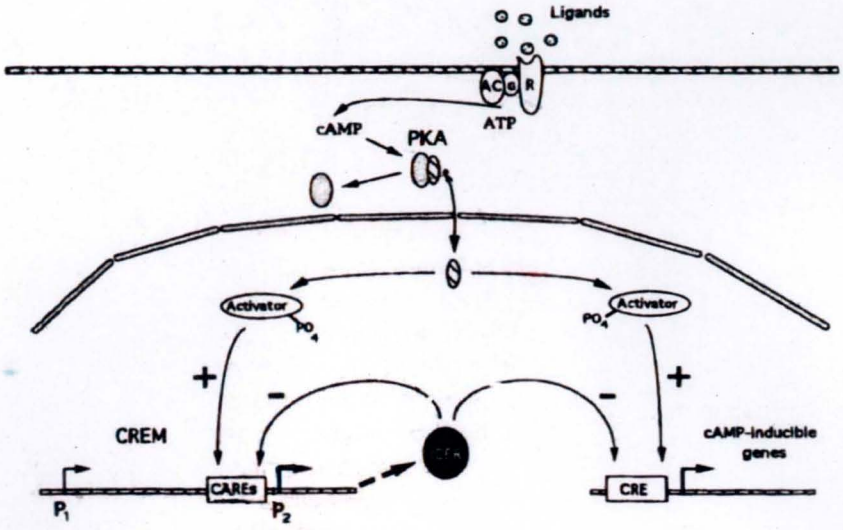

Figure 9 from Molina, C.A., et al., *Inducibility and negative autoregulation of CREM: an alternative promoter directs the expression of ICER, an early response repressor.* Cell, 1993. **75**(5): p. 886.

Figure 4

Number of Mice and Breeding Units

	Wild-type	Transgenic
PTH	**N=10** 1. 0570 2. 0566 3. 0614	**N=10** 1. 0571 2. 0570 3. 0614
Vehicle	**N=10** 1. 0566 2. 0571 3. 0614	**N=7** 1. 0570 2. 0566 3. 0571 4. 0614

Figure 5

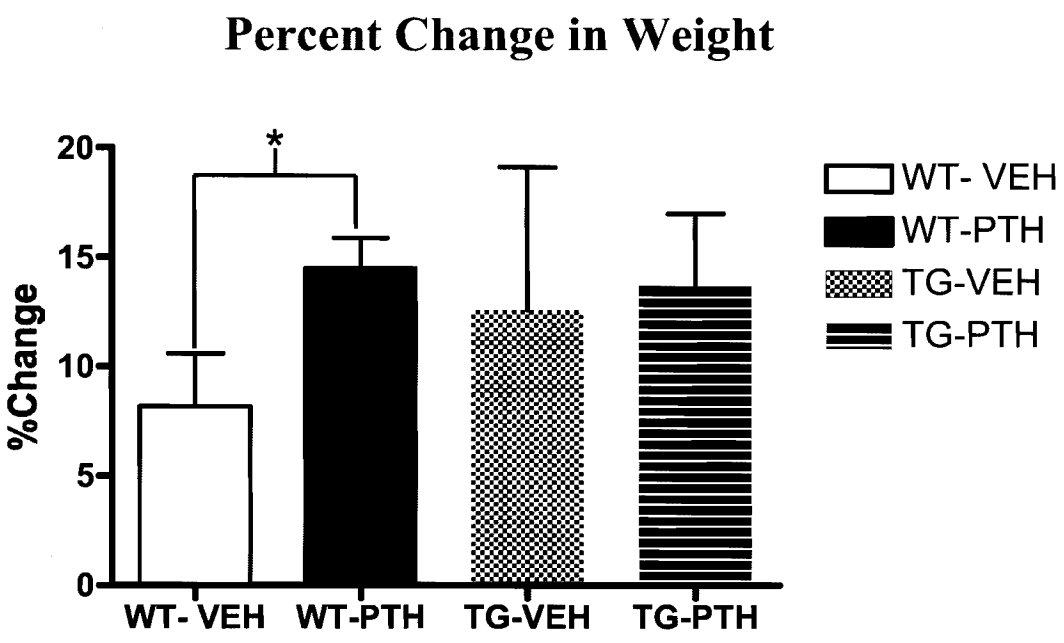
Percent Change in Weight
%Change
20
15
10
5
0
*
WT- VEH
WT-PTH
TG-VEH
TG-PTH
WT- VEH
WT-PTH
TG-VEH
TG-PTH

Figure 6

Wild-type Percent change in Bone Mineral Density

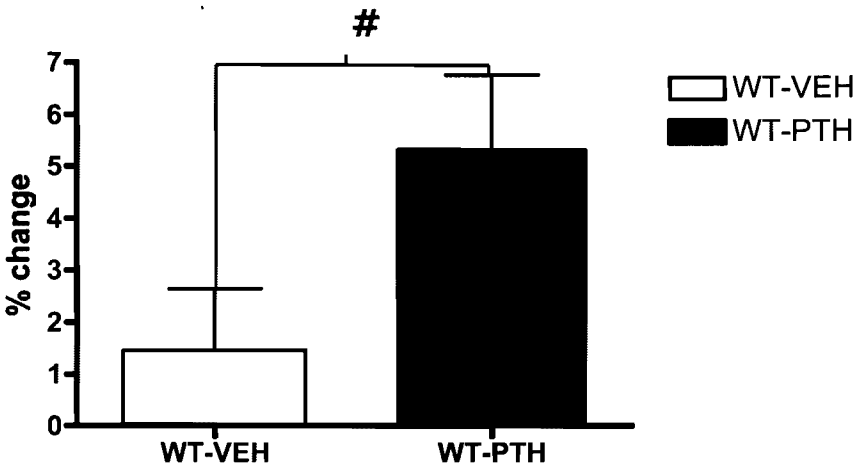

Figure 7

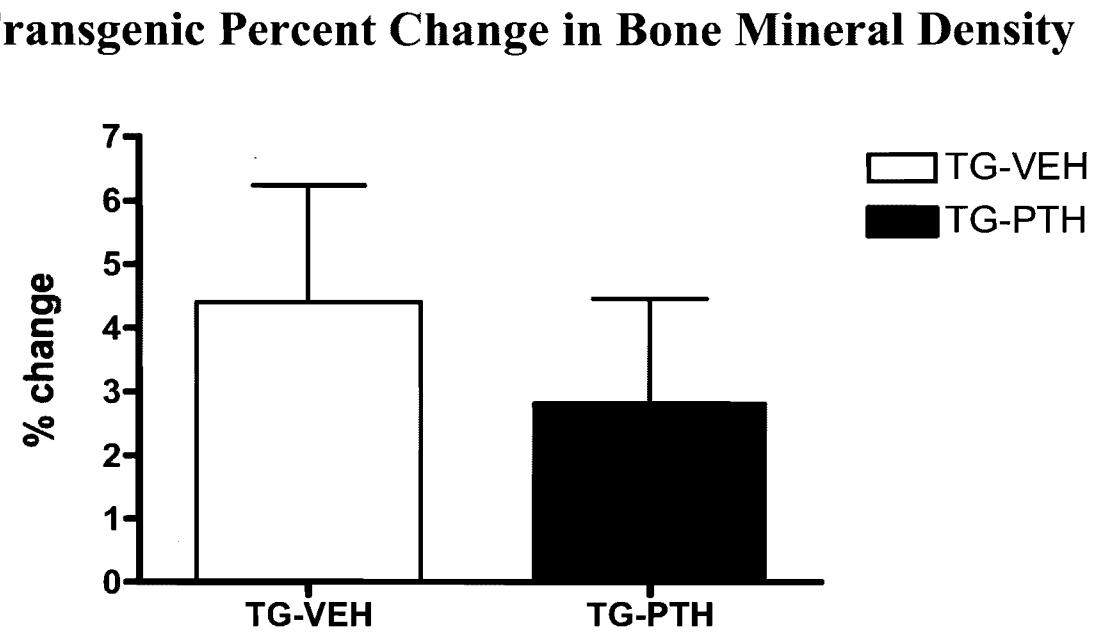
Transgenic Percent Change in Bone Mineral Density
% change
7
6
5
4
3
2
1
0
TG-VEH
TG-PTH
TG-VEH
TG-PTH

Figure 8

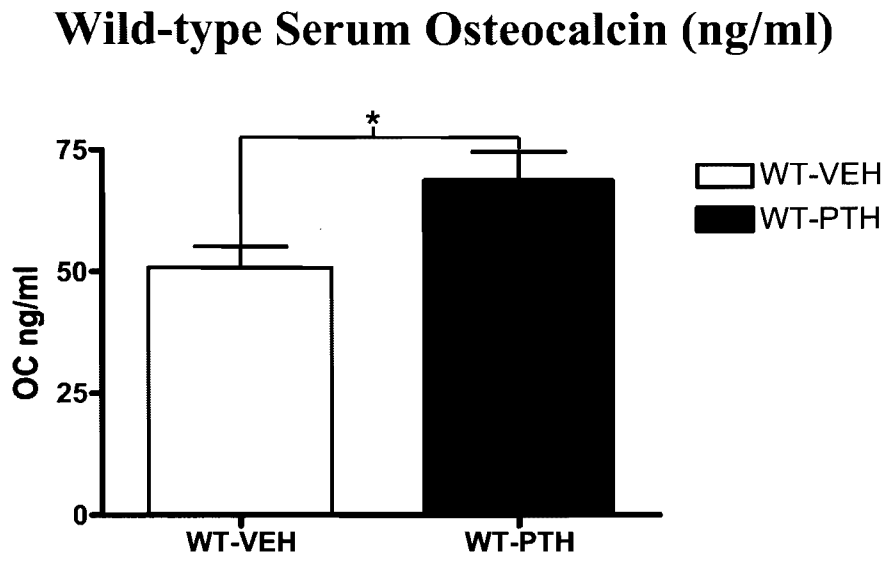
Wild-type Serum Osteocalcin (ng/ml)
*
75
50
25
0
OC ng/ml
WT-VEH
WT-PTH
WT-VEH
WT-PTH

Figure 9

Transgenic Serum Osteocalcin (ng/ml)

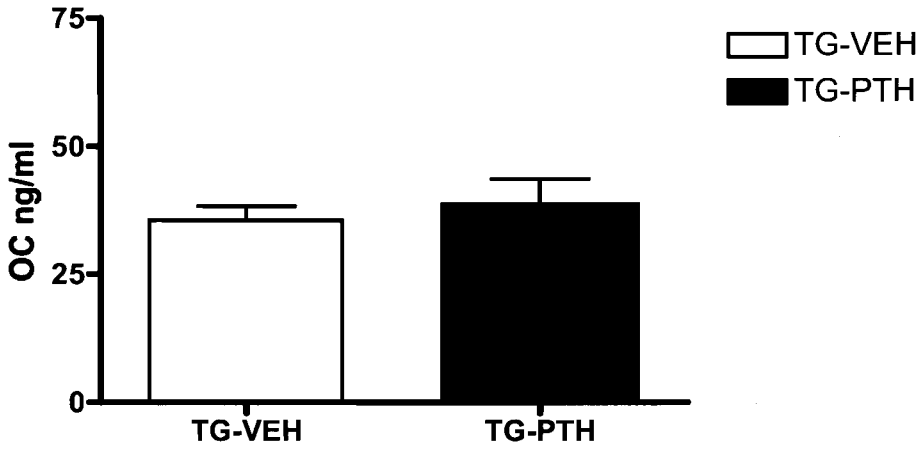

Figure 10

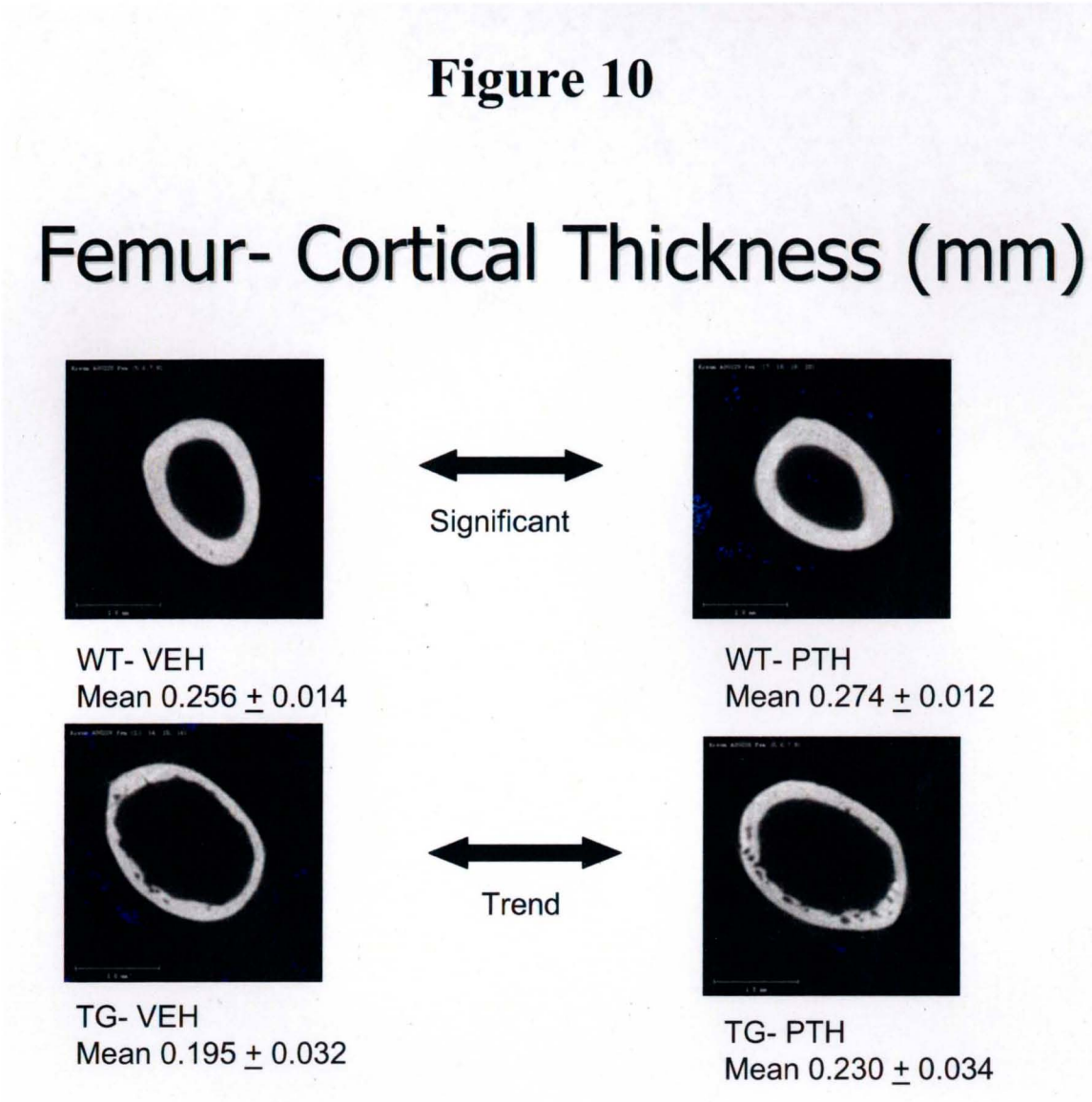
Femur- Cortical Thickness (mm)
Significant
WT- VEH
Mean 0.256 ± 0.014
WT- PTH
Mean 0.274 ± 0.012
Trend
TG- VEH
Mean 0.195 ± 0.032
TG- PTH
Mean 0.230 ± 0.034

Figure 11

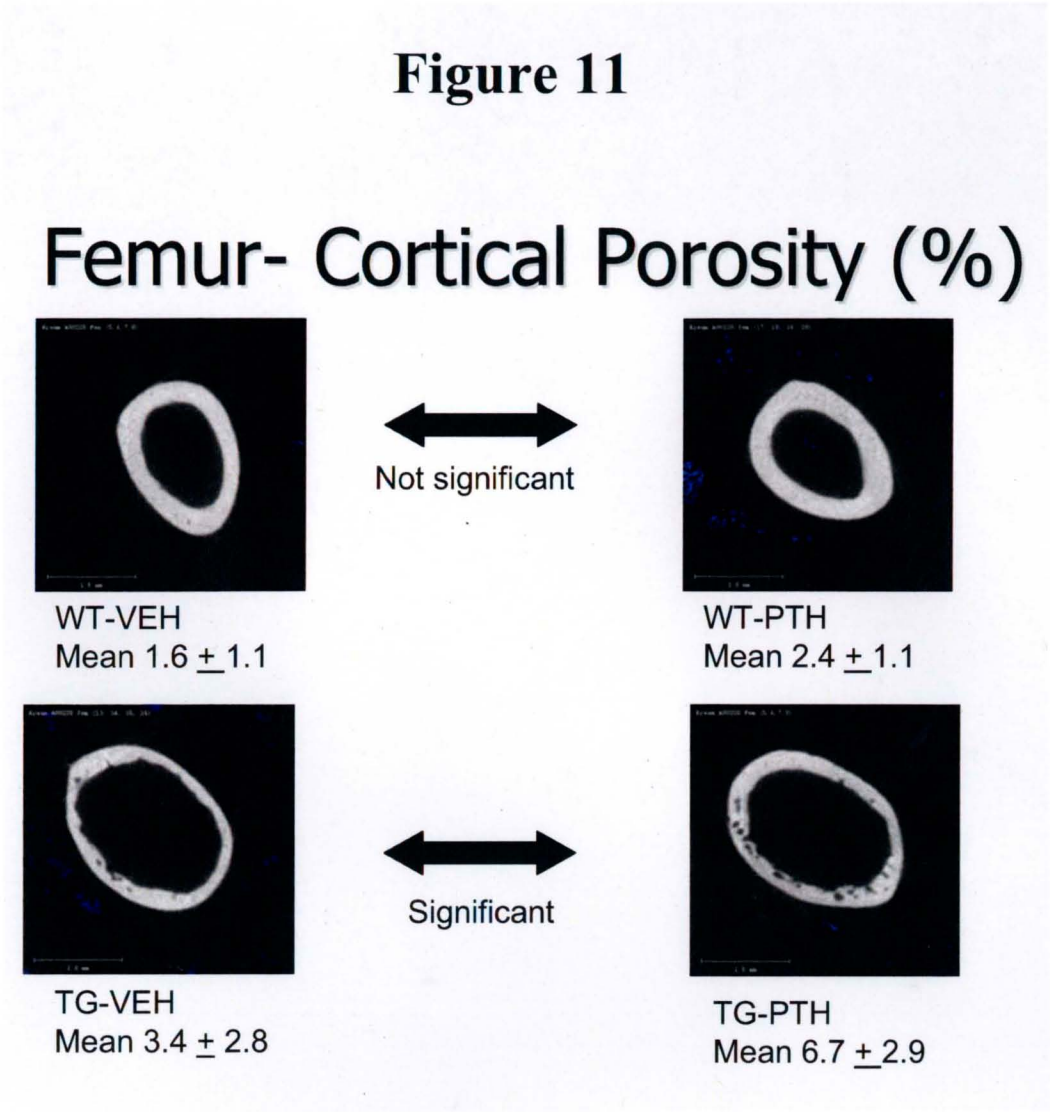
Femur- Cortical Porosity (%)
Not significant
WT-VEH
Mean 1.6 ± 1.1
WT-PTH
Mean 2.4 ± 1.1
Significant
TG-VEH
Mean 3.4 ± 2.8
TG-PTH
Mean 6.7 ± 2.9

Figure 12

Femur- Cortical Bone Area (mm^2)

WT- VEH
Mean 0.992 ± 0.094

Trend

WT- PTH
Mean 1.052 ± 0.061

TG- VEH
Mean 0.803 ± 0.091

significant

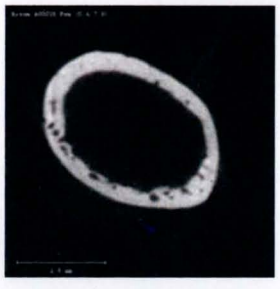

TG- PTH
Mean 0.935 ± 0.130

Figure 13

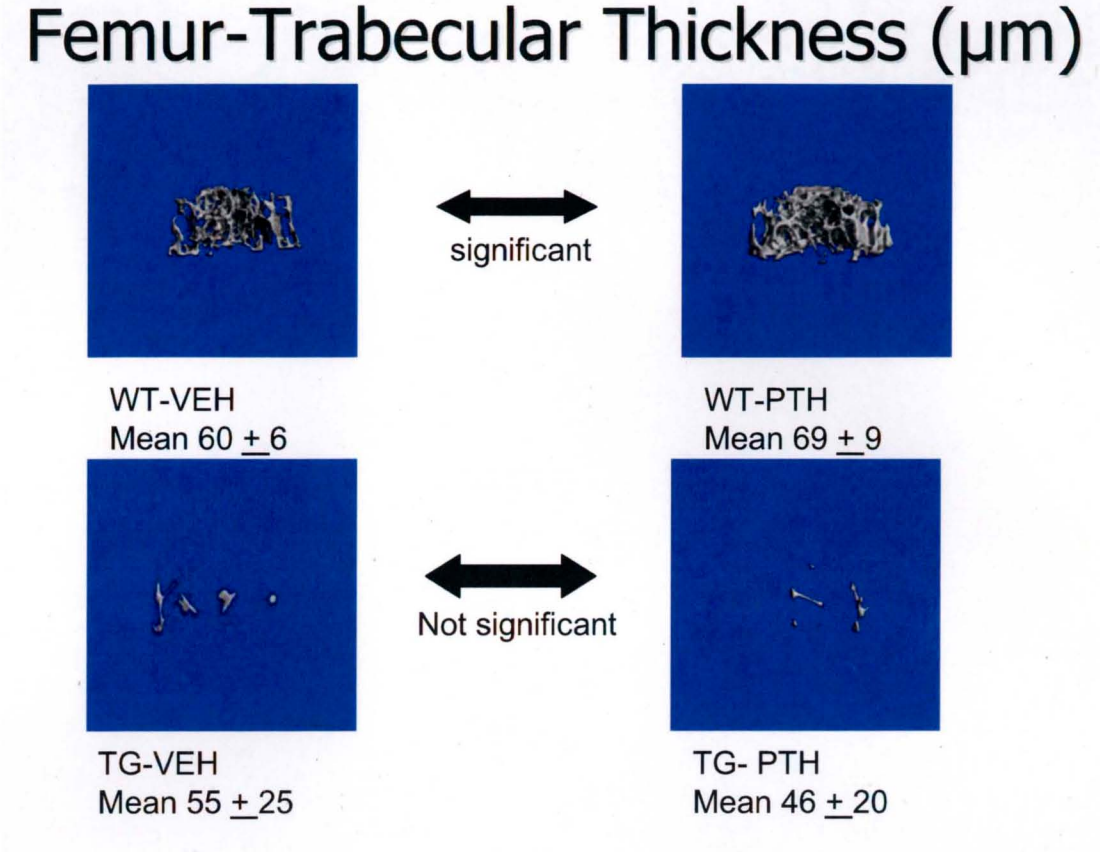
Femur-Trabecular Thickness (μm)
significant
WT-VEH
Mean 60 ± 6
WT-PTH
Mean 69 ± 9
Not significant
TG-VEH
Mean 55 ± 25
TG- PTH
Mean 46 ± 20

Figure 14

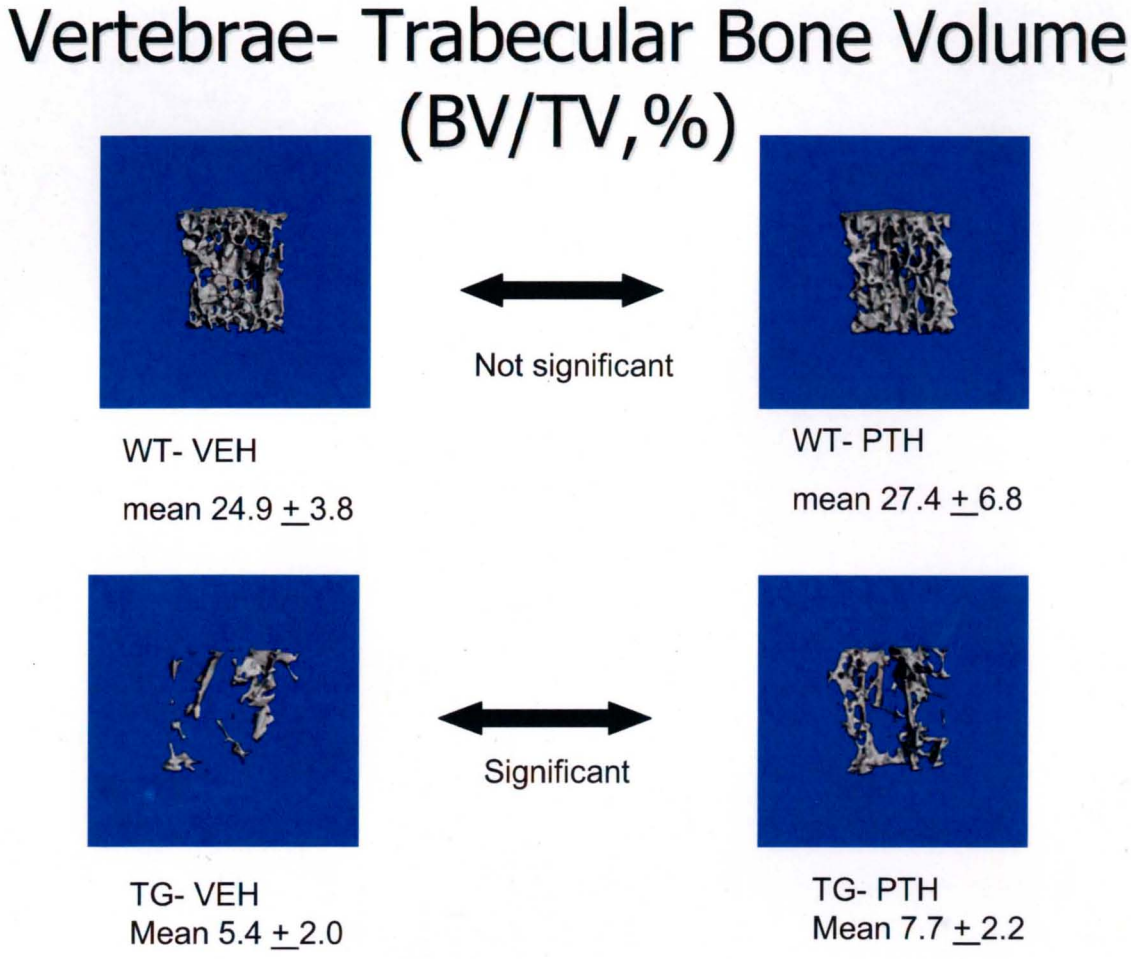
Vertebrae- Trabecular Bone Volume (BV/TV,%)
Not significant
WT- VEH
mean 24.9 ± 3.8
WT- PTH
mean 27.4 ± 6.8
Significant
TG- VEH
Mean 5.4 ± 2.0
TG- PTH
Mean 7.7 ± 2.2

Figure 15

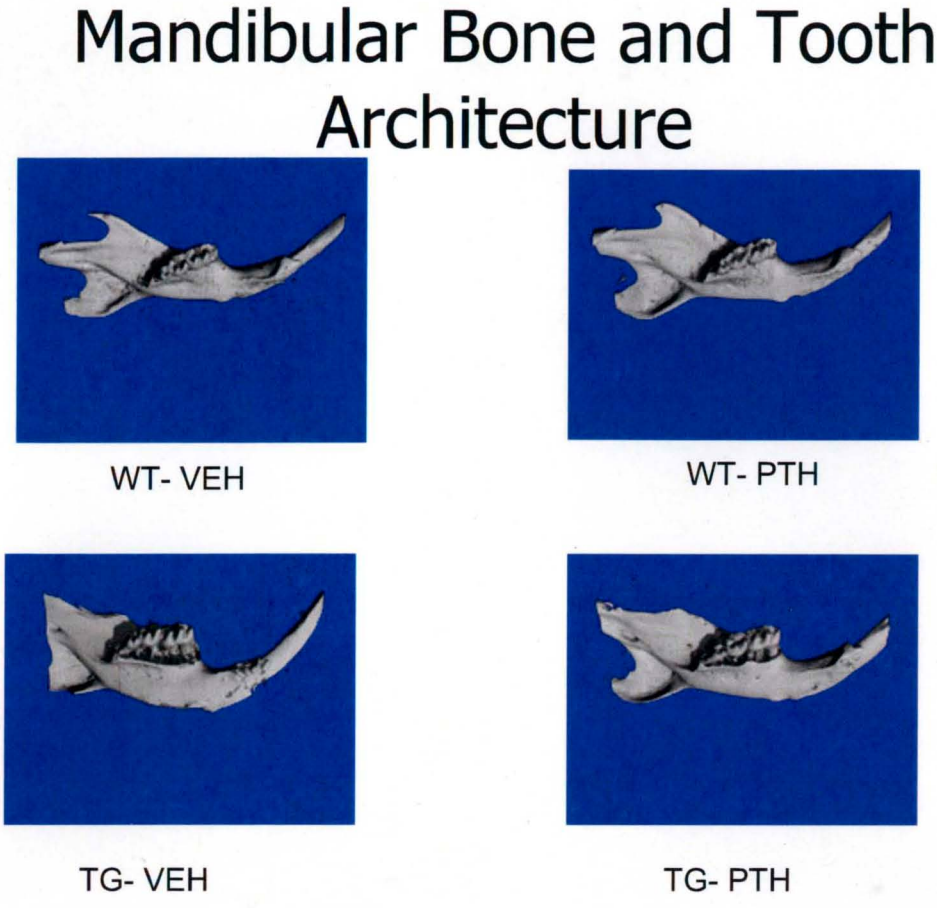
Mandibular Bone and Tooth Architecture
WT- VEH
WT- PTH
TG- VEH
TG- PTH

Figure 16

Mandibles-Cortical Bone Volume(BV/TV) at Level of 1st Molar

WT- VEH
Mean 91.1% ± 1.9

Not significant

WT- PTH
Mean 91.6% ± 1.6

TG- VEH
Mean 74.7% ± 10.2

Not significant

TG- PTH
Mean 72.0% ± 11.6

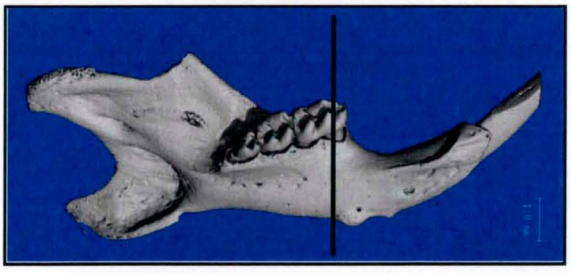

Figure 17

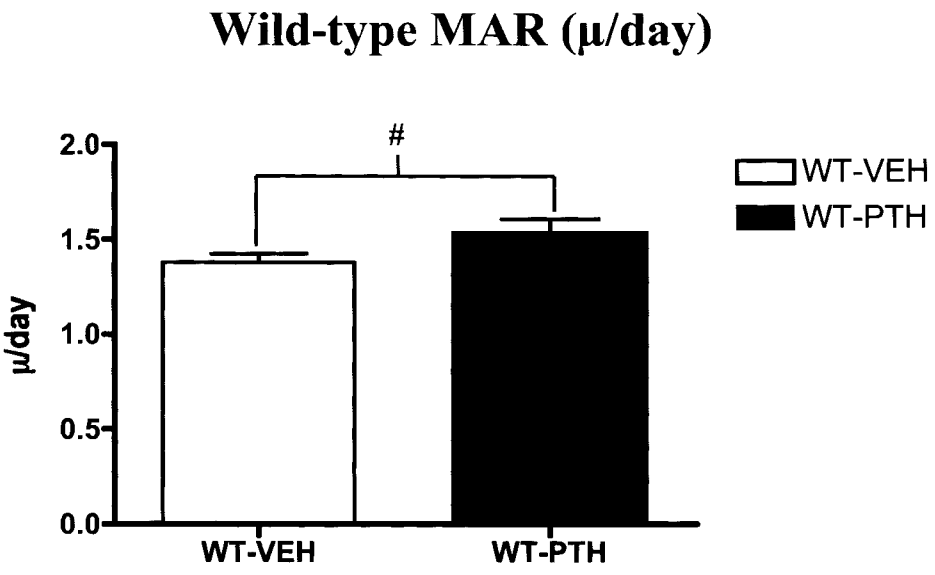

Figure 18

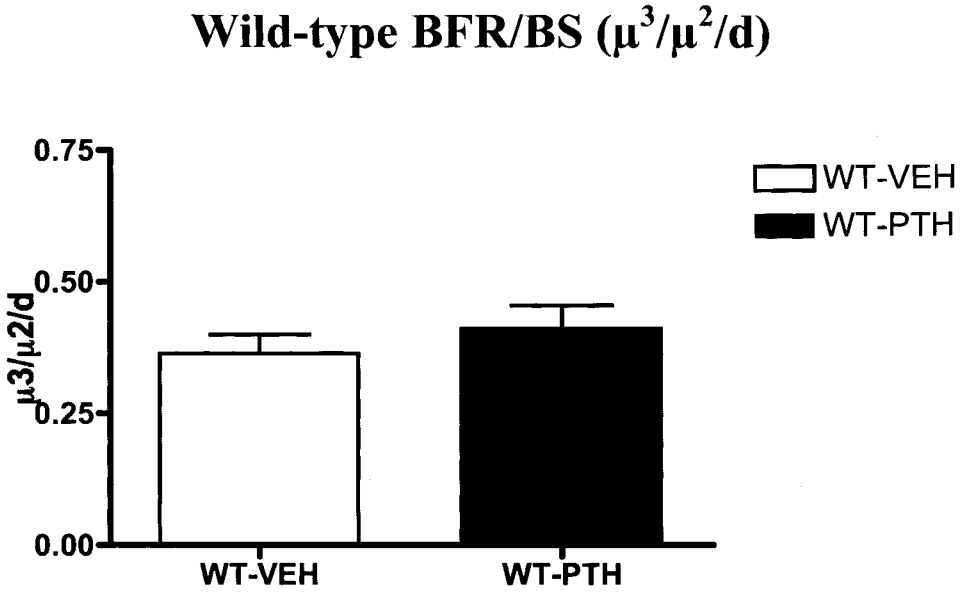
Wild-type BFR/BS (μ³/μ²/d)
0.75
0.50
0.25
0.00
μ3/μ2/d
WT-VEH
WT-PTH
WT-VEH
WT-PTH

Figure 19

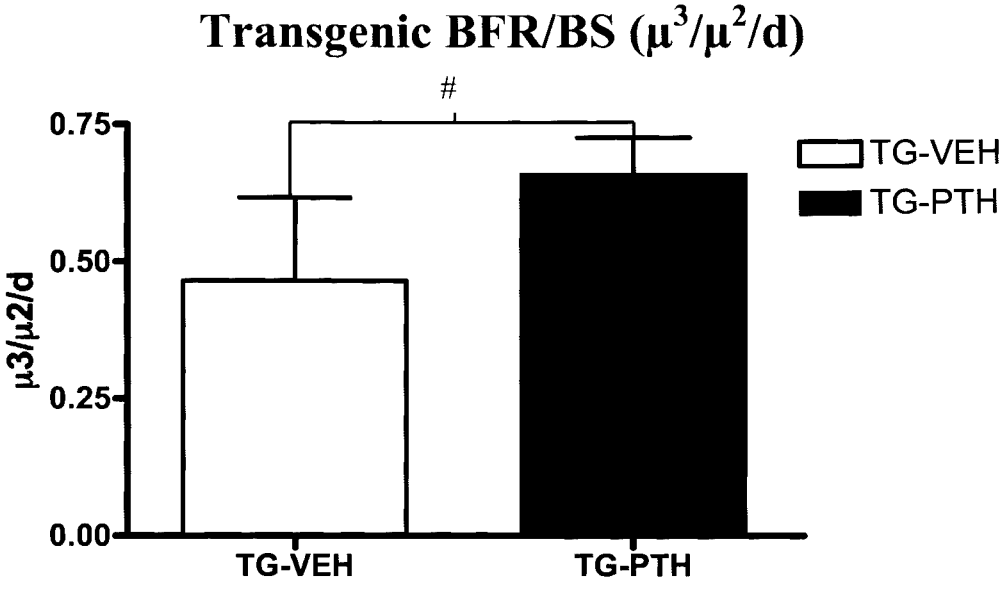
Transgenic BFR/BS (μ³/μ²/d)
#
0.75
0.50
0.25
0.00
μ3/μ2/d
TG-VEH
TG-PTH
TG-VEH
TG-PTH

Figure 20

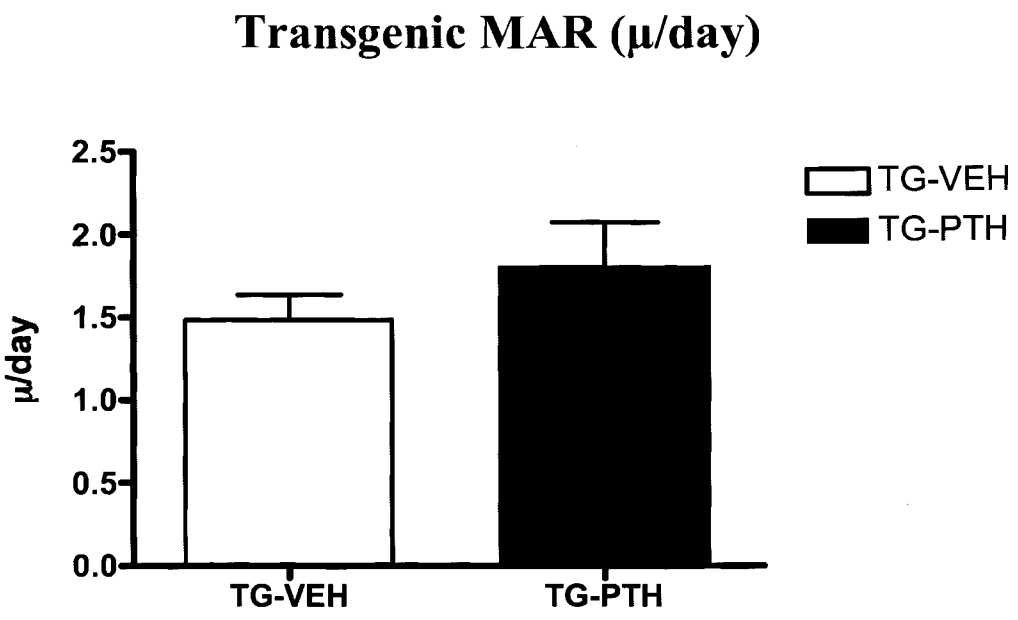
Transgenic MAR (μ/day)
2.5
2.0
1.5
1.0
0.5
0.0
μ/day
TG-VEH
TG-PTH
TG-VEH
TG-PTH

References

1. Molina, C.A., et al., *Inducibility and negative autoregulation of CREM: an alternative promoter directs the expression of ICER, an early response repressor.* Cell, 1993. **75**(5): p. 875-86.

2. Nervina, J.M., et al., *Expression of inducible cAMP early repressor is coupled to the cAMP-protein kinase A signaling pathway in osteoblasts.* Bone, 2003. **32**(5): p. 483-90.

3. Tetradis, S., et al., *Parathyroid hormone induces expression of the inducible cAMP early repressor in osteoblastic MC3T3-E1 cells and mouse calvariae.* J Bone Miner Res, 1998. **13**(12): p. 1846-51.

4. Huang, Y., Chandhoke TK, Liu F, Gronowicz GA, Adams DJ, Harrison JR, Kream BE, *Osteopenia in transgenic mice with osteoblast-targeted expression of the inducible cAMP early repressor.* 2005.

5. Swarthout, J.T., et al., *Parathyroid hormone-dependent signaling pathways regulating genes in bone cells.* Gene, 2002. **282**(1-2): p. 1-17.

6. Cooper, G.M., *The cell: a molecular approach.* third ed. 2004, Washington, DC: ASM Press.

7. Rosen, C.J., *What's new with PTH in osteoporosis: where are we and where are we headed?* Trends Endocrinol Metab, 2004. **15**(5): p. 229-33.

8. Hock, J.M., *Anabolic actions of PTH in the skeletons of animals.* J Musculoskelet Neuronal Interact, 2001. **2**(1): p. 33-47.

9. Seeman, E. and P.D. Delmas, *Reconstructing the skeleton with intermittent parathyroid hormone.* Trends Endocrinol Metab, 2001. **12**(7): p. 281-3.

10. Miller, S.C., et al., *Intermittent parathyroid hormone administration stimulates bone formation in the mandibles of aged ovariectomized rats.* J Dent Res, 1997. **76**(8): p. 1471-6.

11. Iida-Klein, A., et al., *Anabolic action of parathyroid hormone is skeletal site specific at the tissue and cellular levels in mice.* J Bone Miner Res, 2002. **17**(5): p. 808-16.

12. Morrison, K., *Characterization of the mandible and dental phenotype in transgenic mice with osteoblast-targeted overexpression if inducible cAMP early repressor*, in *Department of Medicine and Department of Orthodontics.* 2006, University of Connecticut: Farmington.

13. Gundberg, C.M., M.E. Clough, and T.O. Carpenter, *Development and validation of a radioimmunoassay for mouse osteocalcin: paradoxical response in the Hyp mouse.* Endocrinology, 1992. **130**(4): p. 1909-15.

14. Parfitt, A.M., et al., *Bone histomorphometry: standardization of nomenclature, symbols, and units. Report of the ASBMR Histomorphometry Nomenclature Committee.* J Bone Miner Res, 1987. **2**(6): p. 595-610.

15. Liu, F., et al., *CREM deficiency in mice alters the response of bone to intermittent parathyroid hormone treatment.* Bone, 2007. **40**(4): p. 1135-43.

16. Wang, Y., et al., *Gender differences in the response of CD-1 mouse bone to parathyroid hormone: potential role of IGF-I.* J Endocrinol, 2006. **189**(2): p. 279-87.